

Direct k -space mapping of the electronic structure in an oxide-oxide interface

G. Berner,¹ M. Sing,¹ H. Fujiwara,² A. Yasui,³ Y. Saitoh,³ A. Yamasaki,⁴ Y. Nishitani,⁴ A. Sekiyama,² N. Pavlenko,^{5,6,7} T. Kopp,⁵ C. Richter,^{5,7} J. Mannhart,⁷ S. Suga,⁸ and R. Claessen⁹

¹*Physikalisches Institut and Röntgen Center for Complex Materials Systems (RCCM),
Universität Würzburg, Am Hubland, D-97074 Würzburg, Germany*

²*Division of Materials Physics, Graduate School of Engineering Science, Osaka University, Osaka 560-8531, Japan*

³*Condensed Matter Science Division, Japan Atomic Energy Agency, SPring-8, Hyogo 679-5148, Japan*

⁴*Faculty of Science and Engineering, Konan University, Kobe 658-8501, Japan*

⁵*Center for Electronic Correlations and Magnetism,
Experimental Physics VI, Universität Augsburg, D-86135 Augsburg, Germany*

⁶*Center for Electronic Correlations and Magnetism,
Theoretical Physics III, Universität Augsburg, D-86135 Augsburg, Germany*

⁷*Max Planck Institute for Solid State Research, Heisenbergstraße 1, D-70569 Stuttgart, Germany*

⁸*Institute of Scientific & Industrial Research, Osaka University, Ibaraki, Osaka 567-0047, Japan*

⁹*Physikalisches Institut, Universität Würzburg, Am Hubland, D-97074 Würzburg, Germany*

(Dated: August 27, 2018)

The interface between LaAlO_3 and SrTiO_3 hosts a two-dimensional electron system of *itinerant* carriers, although both oxides are band insulators. Interface ferromagnetism coexisting with superconductivity has been found and attributed to *local* moments. Experimentally, it has been established that Ti $3d$ electrons are confined to the interface. Using soft x-ray angle-resolved resonant photoelectron spectroscopy we have directly mapped the interface states in k -space. Our data demonstrate a charge dichotomy. A mobile fraction contributes to Fermi surface sheets, whereas a localized portion at higher binding energies is tentatively attributed to electrons trapped by O-vacancies in the SrTiO_3 . While photovoltage effects in the polar LaAlO_3 layers cannot be excluded, the apparent absence of *surface-related* Fermi surface sheets could also be fully reconciled in a recently proposed electronic reconstruction picture where the built-in potential in the LaAlO_3 is compensated by *surface* O-vacancies serving also as charge reservoir.

PACS numbers: 79.60.-i, 79.60.Jv, 73.20.-r, 73.50.Pz

Breaking the translational or inversion symmetry at surfaces and interfaces may lead to a rearrangement of charge, spin, orbital, and lattice degrees of freedom. The consequences are particularly interesting in the case of oxides, where already a slight shift in the balance of the respective interactions can stabilize one out of several competing orders or even create novel phases. The case in hand is the formation of a high-mobility two-dimensional electron system (2DES) from Ti $3d$ states at the interface of $\text{LaAlO}_3/\text{SrTiO}_3$ (LAO/STO) heterostructures [1–9] which undergoes a transition into a two-dimensional superconducting state below 0.2 K [4]. However, depending on growth conditions LAO/STO has also been found to display pronounced magnetotransport effects indicating the existence of local moments [12]. More recently, even the simultaneous presence of ferromagnetism and superconductivity has been reported, possibly due to phase separation within the interface [13–16].

The physical origin of the 2DES formation is still debated. The observation that both interface conductivity as well as ferromagnetism only appear for a critical LAO thickness of 4 unit cells (uc) and beyond has been related to electronic reconstruction [2, 15]. In this scenario electrons are transferred from the surface to the interface in order to minimize the electrostatic energy resulting from the polar discontinuity between LAO and STO [3]. Alternative explanations involve doping by oxygen vacancies

[10, 11] and/or cation intermixing [17] but so far have failed to account for the critical thickness. What hampers a better understanding is the lack of microscopic information, in particular on the electronic properties of the interface and the adjacent oxide layers.

Photoelectron spectroscopy is unique in that it can directly probe the single-particle excitations of the valence electrons, which determine the low-energy properties of a solid. Regarding the Ti $3d$ interface electrons in LAO/STO, however, this is hindered for conventional photon energies in the range of 20–100 eV by the insufficient probing depth while in the hard x-ray regime the photoionization cross-sections are too low. Only recently, it has been shown that the Ti $3d$ states can be detected by exploiting the resonance enhancement at the Ti L edge, i.e. by utilizing soft x-rays [8, 9]. Here we use soft x-ray resonant photoelectron spectroscopy (SX-ResPES) to probe the occupied part of the electronic states and in particular its angle-resolved (AR) mode to record Fermi surface (FS) and band maps. Note that the resulting electronic structure may differ from that probed in transport measurements due the additional presence of x-ray induced photocarriers [6, 18].

The LAO/STO heterostructure with a 4 uc thick LAO overlayer was grown at the University of Augsburg by pulsed laser deposition on a TiO_2 -terminated STO substrate. The film thickness was monitored by reflectivity

tion high-energy electron diffraction (RHEED). During growth the oxygen pressure amounted to 1×10^{-4} mbar while the substrate was held at 780°C . Subsequently, the sample was cooled down to room temperature in 0.4 bar of oxygen. Prior to the measurements, the sample surface was cleaned by ozone and gentle *in situ* heating at 180°C [19]. Note that for our samples it has been shown previously that the interface becomes conducting only if a critical thickness of 4 uc is reached [2] and that the highly mobile electrons [20] are confined within a few unit cells on the STO side of the interface where they occupy Ti 3d states [6, 21, 22].

The experiments were performed at the soft X-ray beamline BL23SU of SPring-8 using a photoemission spectrometer equipped with a Gammatdata-Scienta SES-2002 electron analyzer [23] and the fully circularly polarized light from a helical undulator. The energy resolution was set to 110 meV for the angle-integrated and 180 meV for the angle-resolved experiments while the sample temperature was 20 K for all measurements. The angular resolution of the SX-ARPES measurements was 0.2° along and 0.5° perpendicular to the analyzer slit. The Fermi surface map was generated by integrating energy distribution curves at each k -point over an interval of 0.3 eV centered around the Fermi energy. All spectra were corrected for the contribution from second order light [24]. The position of the Fermi level was determined from an *in situ* evaporated gold film [25].

The density functional calculations have been performed using the generalized gradient approximation (GGA+ U) in the Perdew-Burke-Ernzerhof pseudopotential implementation [26] in the QUANTUM ESPRESSO (QE) package [27], with the local Coulomb repulsion U between Ti 3d electrons being 2 eV [28].

In Fig. 1(a) we show angle-integrated ResPES spectra near the chemical potential for a sample with a conducting interface (4uc LAO) upon tuning the photon energy through the Ti L absorption edge. Exciting at a specific absorption edge makes ResPES element-specific. Two processes with the same final state quantum mechanically interfere, namely the direct photoemission and the (coherent and element-specific) Auger emission of the outer valence electrons (involving the direct recombination of a valence electron with the core hole). Thus, any enhancement of spectral weight upon tuning the energy through an absorption edge corresponds to the valence electrons of the respective atomic species, in our case Ti 3d states (for details on ResPES see Supplemental Material, Section I [25]).

The complete valence band spectrum, measured on resonance ($h\nu=460.20\text{eV}$), is depicted in Fig. 1(c). The off-resonance spectrum ($h\nu=445.95\text{eV}$) shows no spectral weight at the chemical potential. Moving through the resonance two structures appear — indicating that both are of Ti 3d character —, a broad structure at a binding energy of $\approx 1.3\text{eV}$ (A) and a structure which is cut off

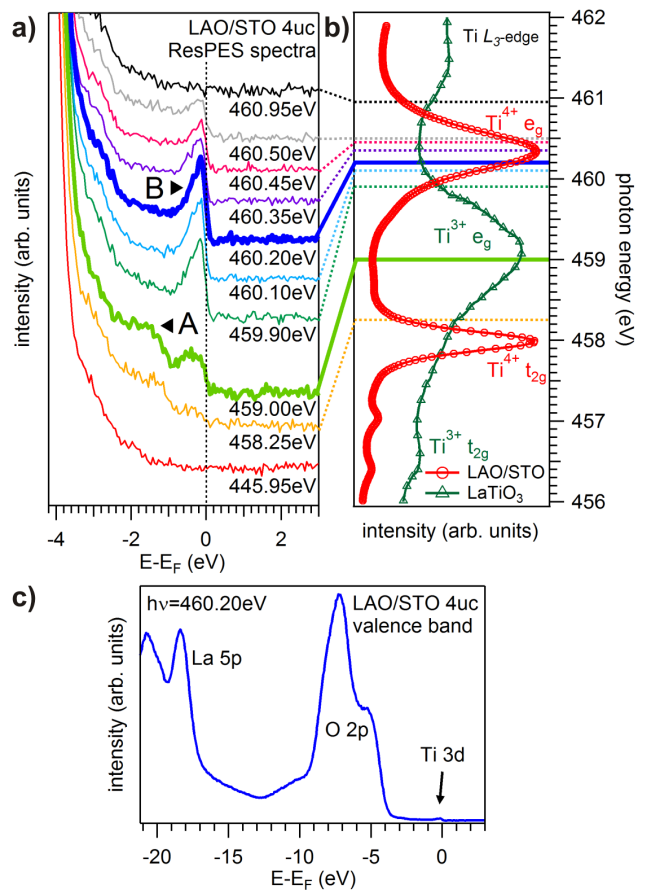


FIG. 1. (Color online) (a) Angle-integrated resonant photoemission spectra upon tuning the photon energy through the Ti L absorption edge. (b) Ti L absorption spectra, recorded in total electron yield mode, of LAO/STO (red) and LaTiO_3 (green, taken from Ref. [7]). The photon energies used in the measurements displayed in (a) are indicated by dashed and solid lines. (c) On-resonance photoemission spectrum, displaying the complete valence band.

by the Fermi-Dirac distribution function [marked by B in Fig. 1 (a)] and hence is tentatively ascribed to metallic states. Interestingly, the two features A and B resonate at different photon energies which already signals that they originate from different types of electronic states.

To get further insight, one has to relate the ResPES excitation energies to their positions on the resonance curve, i.e. the x-ray absorption spectrum [Fig. 1(b)]. The spectrum to compare with is that of a reference sample representative for Ti in a 3+ oxidation state, here LaTiO_3 (green), while for LAO/STO (red) the absorption is dominated by the Ti^{4+} ions of the substrate. Peak A resonates exactly on the absorption maximum (associated with the so-called e_g levels) of LaTiO_3 (Ti^{3+}) whereas the maximum enhancement of B is delayed by $\approx 1\text{eV}$ to almost the following absorption minimum. In addition, feature B resonates over a wider energy range than

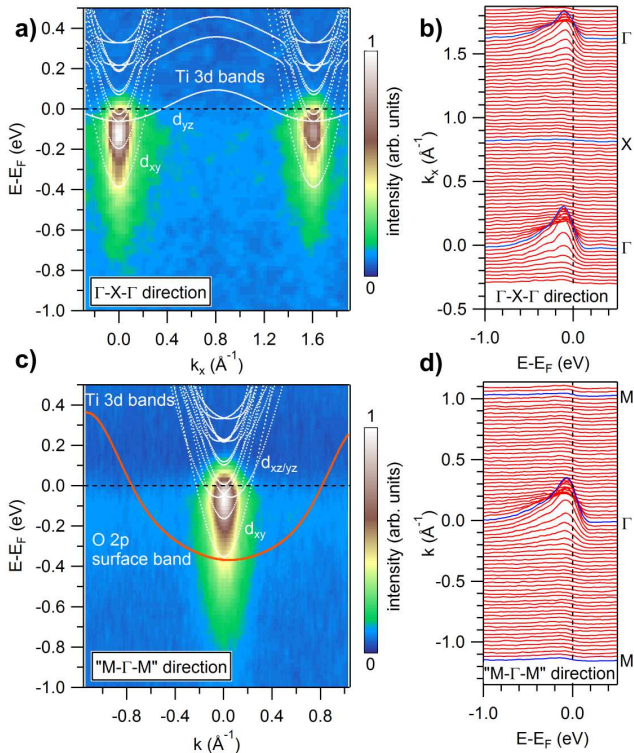


FIG. 2. (Color online) (a) Band map along the Γ -X- Γ line of the BZ. (b) Same data as in (a) depicted as energy distribution curves. (c) Band map along a cut close to the M- Γ -M line of the BZ (hence denoted by "M- Γ -M"). (d) Same data as in (c), depicted as energy distribution curves. All data were taken at $h\nu = 460.20$ eV. White and red lines represent theoretical band dispersions (for details see text).

feature *A*. This phenomenology is known from ResPES on transition metals [29] and indicates that features *A* and *B* should originate from localized and delocalized states, respectively [25]. While the delocalized states (*B*) are readily identified as Ti 3*d* band states, forming the 2DES, we assign the localized states (*A*) to Ti 3*d* impurity states. Such trapped states are likely to be induced by O vacancies adjacent to Ti ions. Our recent band structure calculations based on density-functional theory (DFT) reveal similar peaks in the density of states between -2 eV and -1 eV, depending on O vacancy configuration and concentration [16]. Similar observations have been reported for scanning tunneling spectroscopy measurements on LAO/STO [30] and PES experiments on bare STO surfaces [31, 32], where the spectral weight at the chemical potential and the in-gap states around -1.3 eV were discussed in terms of coherently screened and poorly screened excitations [32], respectively.

Since momentum information is still preserved in valence band photoemission using soft x-rays and due to the resonance enhancement at the Ti *L* edge we have been able to perform *k*-space mapping of the 2DES interface states [Figs. 2(a) and (c)]. In Figs. 2(b) and (d)

we display the corresponding *k*-resolved energy dispersion curves along the Γ -X- Γ direction and a cut close to the M- Γ -M line [see dashed lines in Fig. 3(b)]. One clearly observes states dispersing with *k* around Γ and an occupied band width of ≈ 0.4 eV, conclusively confirming our tentative assignment from above to the metallic interface band states of the 2DES. In Figs. 2(a) and (c), the electronic dispersions of DFT calculations are overlaid. The calculations fairly reproduce the experimental band width, while the experimental broadening does not allow us to resolve all the individual quantum well states owing to the confinement of the 2DES [33], although the energy distribution curves in Figs. 2(b) and (d) indicate the existence of at least two bands.

Additional information can be extracted from the FS map in Fig. 3. An essentially isotropic distribution of high intensity centered at the Γ points of the BZ is observed. Superimposed one finds, with much lower intensity, flower-shaped spectral weight with the lobes directed towards the X points of the BZ and stretching further out than the isotropic intensity distribution as is most clearly seen around the lower left Γ point in Fig. 3(a). These observations are in line with the FS sheets from the DFT calculations which are overlaid on top of the PES data in Fig. 3(b). Note, however, that the experimental Fermi surface volume might be slightly enhanced due to photo-generated charge carriers [6]. The calculations further reveal that the isotropic intensity distribution originates mainly from light Ti 3*d*_{*xy*} bands while the flower-shaped intensity distribution is due to heavy *d*_{*xz*}/*d*_{*yz*} [Fig. 2] bands, similar to what has recently been reported for a 2DES at the surface of bare STO [33].

However, there is also a striking discrepancy between experiment and theory. In the calculations, which are performed for stoichiometric samples, i.e., in the absence of oxygen vacancies in the LAO, a hole-like FS is predicted around the M points as indicated by the orange dashed lines in Fig. 3(b). It is due to the Fermi level crossing of O 2*p* derived states from the valence band maximum of the topmost monolayer of the LAO film. Since the photoelectron current emitted from the surface is hardly damped by scattering events and since the band is almost completely filled, these hole pockets, if existing, should be observable even without resonance enhancement. In the standard electronic reconstruction scenario [Fig. 4(a)] the polarity-induced potential build-up across the overlayer gradually shifts the valence band of LAO towards the Fermi level. At the critical thickness, the valence band maximum crosses the Fermi level which gives rise to the hole pockets predicted by the DFT calculations, while the released electrons populate the lowest lying Ti 3*d* states at the STO side of the interface [34].

From the obvious absence of metallic surface bands we conclude that the potential difference is (almost completely) screened out in the LAO film [35]. A possible

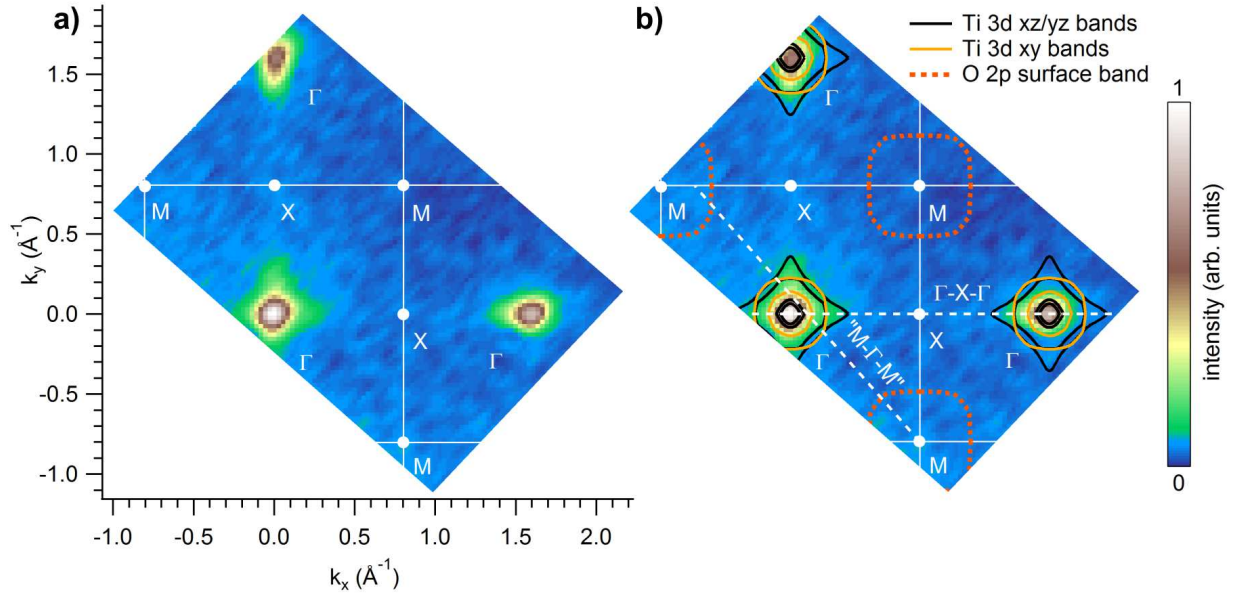


FIG. 3. (Color online) (a) FS map recorded at $h\nu = 460.20$ eV. (b) Same map as (a) but with the cuts in the BZ corresponding to the data in Fig. 2(a)-(d) indicated and the FS sheets from DFT calculations overlaid.

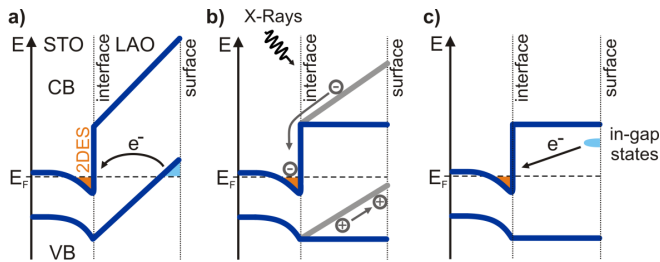


FIG. 4. (Color online) (a) Schematic band diagram for the standard electronic reconstruction scenario in LAO/STO. (b) Possible situation where the polarization field in the LAO is screened by the separation of electron-hole pairs created upon illumination with x-rays. (c) Tentative band situation with the inclusion of O vacancies at the LAO surface as charge reservoir for electronic reconstruction.

explanation could be that under illumination electron-hole pairs are created which get separated by the initial polarization field in the LAO [Fig. 4(b)]. Eventually, depending on the rates for electron-hole pair creation and recombination a dynamic equilibrium will be established where the opposing electric field due to the separated electron-hole pairs just cancels the initial field, thus prohibiting the observation of the surface related hole pocket. On the other hand, in another polar/non-polar heterostructure ($\text{LaCrO}_3/\text{SrTiO}_3$) a built-in potential has readily been identified by x-ray photoelectron spectroscopy (XPS) with a similar potential drop per uc as predicted for LAO/STO in the standard electronic reconstruction scenario [36].

Looking for alternative explanations, our SX-ARPES results could also be fully reconciled within recent proposals, also based on DFT calculations, that oxygen vacancies at the LAO surface can serve as charge reservoir for the electronic reconstruction [37–40]. In such a scenario the O vacancies induce unoccupied in-gap states, which due to possible disorder of the vacancies in the real system might easily become localized. The released two electrons per O vacancy are transferred to the interface by the LAO polar field. This field is thereby efficiently reduced [see Fig. 4(c)], in line with XPS measurements which show no core-level broadening or shift with film thickness [41].

Viewing the LAO film as a parallel plate capacitor the energy gain per charge transferred from the surface to the interface increases linearly with film thickness. While the energy costs for the creation of oxygen vacancies can depend also on thickness (and in addition on vertical position), the calculations show that at a certain thickness it becomes on balance favorable to create an oxygen vacancy at the surface and transfer the released electrons to the interface [37–40]. Note that O vacancies in the STO can be excluded with fair certainty as source of electrons for the 2DES. First, their density essentially does not depend on film thickness but on the growth conditions and so the critical thickness behavior as observed in our samples could hardly be explained [2]. Second, in our data the electrons associated with O vacancies in the STO (feature A) are well separated and far below the 2DES related states at the chemical potential (feature B) and thus cannot populate the 2DES related states.

Summarizing our results we arrive at the picture that at the conducting interface besides heavy Ti $3d_{xz/yz}$ and light Ti $3d_{xy}$ bands there also exist *localized* charge carriers of Ti $3d$ character. These are probably trapped by adjacent O vacancies, i.e. O vacancies in the STO at the interface. It is hence tempting to associate the trapped and mobile interface charge with ferromagnetism and superconductivity, respectively [16], which both have recently been reported to coexist at the interface. As a matter of fact, the hallmarks of the microscopic view of the standard electronic reconstruction scenario — a metallic surface and a potential drop across the LAO overlayer of the order of the STO band gap — experimentally remained elusive so far. Our data clearly indicate that they are absent in our spectroscopic experiments. Modified electronic reconstruction scenarios involving surface O vacancies as charge reservoir could explain these findings. Since we cannot rule out the possibility that the LAO polar field is screened out by a photoinduced reverse voltage our results call for both a systematic investigation of scenarios taking O vacancies into account and combined *in situ* transport and spectroscopy experiments. In any case, these results demonstrate for the first time that SX-ARPES can provide valuable k -space information on the electronic structure of *buried* interfaces.

We are grateful to T. Kiss for setting-up and optimizing the ARPES spectrometer and C. Hughes for help with the sample preparation. This work was supported by the Deutsche Forschungsgemeinschaft (FOR 1162 and TRR 80), the German Federal Ministry for Education and Research (05 K10WW1) and by the Grant-in-Aid for Innovative Areas (20102003) "Heavy Electrons" from MEXT, Japan. The measurements were performed under the Shared Use Program of JAEA Facilities (Proposal No. 2011B-E31) and the approval of BL23SU at SPring-8 (Proposal No. 2011B3820). HF was supported by MEXT/JSPS KAKENHI Grant Number 23740240.

- [18] It is known that ultraviolet light illumination with energies exceeding the STO band gap causes photoconductivity in LAO/STO samples [M. Huijben *et al.*, Nature Mater. **5**, 556 (2006)]. Using even higher photon energies in SX-PES obviates the need for keeping the samples in the dark prior to the experiments as is done e.g. in transport measurements to avoid photocarrier contributions.
- [19] See Supplemental Material, Section III, at [URL will be inserted by publisher]
- [20] C. W. Schneider *et al.*, Appl. Phys. Lett. **89**, 122101 (2006).
- [21] G. Berner *et al.*, Phys. Rev. B **82**, 241405 (2010).
- [22] K.-J. Zhou *et al.*, Phys. Rev. B **83**, 201402 (2011).
- [23] Y. Saitoh *et al.*, J. Synchrotron Rad. **19**, 388 (2012).
- [24] See Supplemental Material, Section II, at [URL will be inserted by publisher]
- [25] See Supplemental Material, Section I, at [URL will be inserted by publisher]
- [26] J. P. Perdew *et al.*, Phys. Rev. Lett. **77**, 3865 (1996).
- [27] P. Giannozzi *et al.*, J. Phys.: Condens. Matter **21**, 395502 (2009).
- [28] See Supplemental Material, Section IV, at [URL will be inserted by publisher]
- [29] T. Kaurila *et al.*, J. Phys.: Condens. Matter **9**, 6533 (1997).
- [30] Z. Ristic *et al.*, Phys. Rev. B **86**, 045127 (2012).
- [31] Y. Aiura *et al.*, Surf. Sci. **515**, 61 (2002).
- [32] Y. Ishida *et al.*, Phys. Rev. Lett. **100**, 056401 (2008).
- [33] A. F. Santander-Syro *et al.*, Nature **469**, 189 (2011).
- [34] R. Pentcheva *et al.*, Phys. Rev. Lett. **102**, 107602 (2009).
- [35] The leading edge of the O $2p$ -derived states (originating from both LAO and STO) in Fig. 1(b) indicates an energy gap of about 3.2 eV, corresponding within experimental accuracy to the STO band gap. If there was a sizeable potential difference across the LAO left the gap of the leading edge (then originating solely from LAO) would have to be significantly reduced.
- [36] S. A. Chambers *et al.*, Phys. Rev. Lett. **107**, 206802 (2011).
- [37] Z. Zhong *et al.*, Phys. Rev. B **82**, 165127 (2010).
- [38] N. C. Bristowe *et al.*, Phys. Rev. B **83**, 205405 (2011).
- [39] Y. Li *et al.*, Phys. Rev. B **84**, 245307 (2011).
- [40] N. Pavlenko *et al.*, Phys. Rev. B **86**, 064431 (2012).
- [41] Y. Segal *et al.*, Phys. Rev. B **80**, 241107 (2009).

-
- [1] A. Ohtomo *et al.*, Nature **427**, 423 (2004).
- [2] S. Thiel *et al.*, Science **313**, 1942 (2006).
- [3] N. Nakagawa *et al.*, Nature Mater. **5**, 204 (2006).
- [4] N. Reyren *et al.*, Science **317**, 1196 (2007).
- [5] M. Basletic *et al.*, Nature Mater. **7**, 621 (2008).
- [6] M. Sing *et al.*, Phys. Rev. Lett. **102**, 176805 (2009).
- [7] M. Salluzzo *et al.*, Phys. Rev. Lett. **102**, 166804 (2009).
- [8] G. Drera *et al.*, Appl. Phys. Lett. **98**, 052907 (2011).
- [9] A. Koitzsch *et al.*, Phys. Rev. B **84**, 245121 (2011).
- [10] W. Siemons *et al.*, Phys. Rev. Lett. **98**, 196802 (2007).
- [11] A. Kalabukhov *et al.*, Phys. Rev. B **75**, 121404 (2007).
- [12] A. Brinkman *et al.*, Nature Mater. **6**, 493 (2007).
- [13] L. Li *et al.*, Nature Phys. **7**, 762 (2011).
- [14] J. A. Bert *et al.*, Nature Phys. **7**, 767 (2011).
- [15] B. Kalisky *et al.*, Nature Comm. **3**, 922 (2012).
- [16] N. Pavlenko *et al.*, Phys. Rev. B **85**, 020407 (2012).
- [17] P. R. Willmott *et al.*, Phys. Rev. Lett. **99**, 155502 (2007).

SUPPLEMENTAL INFORMATION

RESONANT PHOTOELECTRON SPECTROSCOPY (RESPES) – TECHNIQUE AND DATA NORMALIZATION

Photoemission (PES) from the Ti $3d$ interface states can only be accomplished with reasonable intensity, if one takes advantage of the resonance enhancement at the Ti L absorption edge. With the photon energy tuned to the absorption threshold, a second path opens how to arrive at the same final state as in the direct photoemission process [Fig. 5(a)]:

$$2p^6 3d^n \rightarrow 2p^6 3d^{n-1} + \epsilon \quad (\text{direct PES}), \quad (1)$$

$$2p^6 3d^n \rightarrow 2p^5 3d^{n+1} \rightarrow 2p^6 3d^{n-1} + \epsilon \quad (\text{Auger decay}), \quad (2)$$

where ϵ denotes the ejected photoelectron. This second path involves the dipole excitation of an electron from the Ti $2p$ into the Ti $3d$ shell and a subsequent Auger-like decay (often called direct recombination), resulting in the ejection of a $3d$ electron and a filled $2p$ shell. The probability amplitudes of both channels interfere quantum mechanically and give rise to a resonance enhancement of only the $3d$ spectral weight [1]. This picture is based on an atomic description of the $3d$ electrons. Note that in the case of metallic (Bloch-like) electrons in a solid the simple situation as sketched in Fig. 5(a) might be refined. By hybridization, neighboring atoms interact and the discrete atomic levels broaden into wide bands. In ResPES, part of the energy of the initial photon now can be stored in a broad continuum of excitations between occupied and unoccupied band states, leading to a delayed resonance maximum and a stretched resonance range. Such a behavior is known from transition metals [2] and also observed here.

All spectra were normalized in intensity to the non-resonating La $5p$ core-level intensity at -18.4eV [see Fig. 5(b)]. The energy scale was calibrated at the Fermi level as determined from a gold film which has been freshly evaporated on the metallic sample carrier beside the sample after the measurements. By shorting the two-dimensional electron system (2DES) and the grounded sample carrier with silver paint applied to the side faces of the sample, we ensured that also the 2DES is in galvanic contact with the spectrometer and hence 2DES and Au film share the same chemical potential.

CORRECTION FOR 2nd ORDER CONTRIBUTIONS

Significant intensity from the Ti $2p_{3/2}$ core level excited by 2nd order light appeared in all spectra in the

region around the chemical potential [see Fig. 6(a)] although the 2nd order light is much weaker than the intensity of the 1st harmonic due to the use of the circularly polarized light from a helical undulator. For spectra measured at photon energies between 459.90eV and 460.95eV the 2nd order light induced peak was fitted by a Gaussian line and subtracted from both the angle-integrated and angle-resolved spectra.

For the spectra measured at lower photon energies (445.95eV , 458.25eV and 459.00eV) the 2nd order peak overlaps with 1st order spectral weight below the chemical potential. It was subtracted by using the Gaussian lineshape observed at higher photon energies and accounting for the $2\Delta h\nu$ shift of second order light, if the fundamental photon energy changes by $\Delta h\nu$. The second order excitation of the Ti $2p$ electrons also allowed for an absolute calibration of the photon energies used in photoemission and x-ray absorption.

SAMPLE SURFACE PREPARATION

For the measurements a clean sample surface is essential to minimize scattering of the photoelectrons and optimize the signal-to-noise ratio of the spectra. The sample was transported under air to the synchrotron radiation laboratory. Prior to the measurements the sample was kept under ozone flow for 45 min, followed by an *in situ* annealing at 180°C under 1×10^{-5} mbar of oxygen for 45 min. After this procedure a high quality LEED pattern with a 1×1 surface is observed [see Fig. 6(b)], signalling a clean and long-range ordered LAO surface. The lattice constant inferred from this pattern is $(3.97 \pm 0.1)\text{\AA}$, which is within the error bars in good agreement with the lattice constant of STO (3.905\AA). No surface reconstruction was found.

DENSITY FUNCTIONAL CALCULATIONS

Density functional calculations have been performed using the generalized gradient approximation (GGA+ U) in the Perdew-Burke-Ernzerhof pseudopotential implementation [3] in the QUANTUM ESPRESSO (QE) package [4]. The local Coulomb repulsion U between Ti $3d$ electrons was chosen to be 2eV .

A number of supercells consisting of two symmetric LAO/STO parts were generated, where each part contains a stack of 4 uc thick LAO layers on a 3.5 uc thick STO slab. The interfacial configuration is considered as TiO_2/LaO . The LAO-STO-LAO parts are separated by a 13\AA -thick vacuum sheet. A kinetic energy cutoff of 640eV and the Brillouin zone (BZ) of the 106-to 166-atom supercells sampled with $5 \times 5 \times 1$ to $9 \times 9 \times 1$ k -point grids are used. For the stoichiometric vacancy-free structures, the electronic state can be characterized as

metallic, with the interface electron charge emerging due to the compensation of the polar field across the LAO. The number of electrons per (1×1) uc transferred to the t_{2g} states of the TiO_2 -layers at the interface amounts to 0.34.

-
- [1] S. Hüfner, *Photoelectron spectroscopy: principles and applications* (Springer (Berlin, Heidelberg), 2003), 3rd ed.
 - [2] T. Kaurila *et al.*, *J. Phys.: Condens. Matter* **9**, 6533 (1997).
 - [3] J. P. Perdew *et al.*, *Phys. Rev. Lett.* **77**, 3865 (1996).
 - [4] P. Giannozzi *et al.*, *J. Phys.: Condens. Matter* **21**, 395502 (2009).

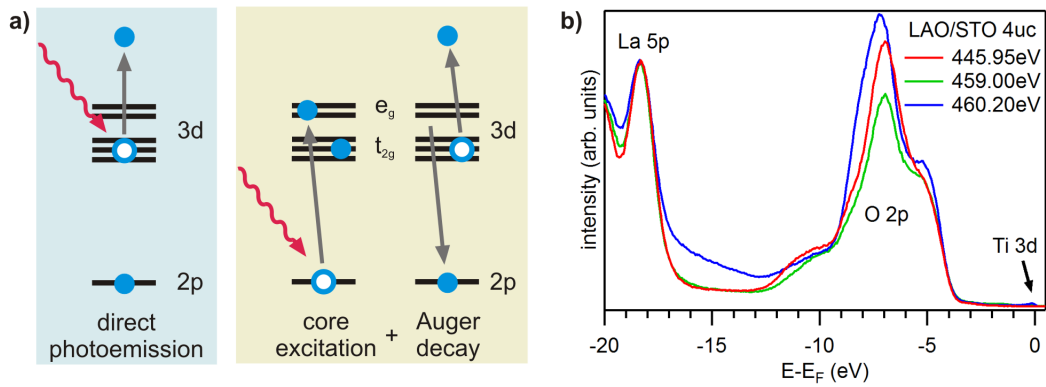


FIG. 5. (Color online) Resonant enhancement in photoemission and data normalization. (a) Sketch of the two excitation channels which quantum mechanically interfere in resonant photoemission. (b) The spectra have been normalized to the non-resonating La 5p core-level as is shown here for spectra measured at $h\nu = 445.95$ eV (off-resonance), $h\nu = 459.00$ eV (Ti^{3+} e_g resonance), and $h\nu = 460.20$ eV (on-resonance for Fermi surface mapping). The resonance enhancement in the O 2p region is due to the O 2p - Ti 3d hybridization.

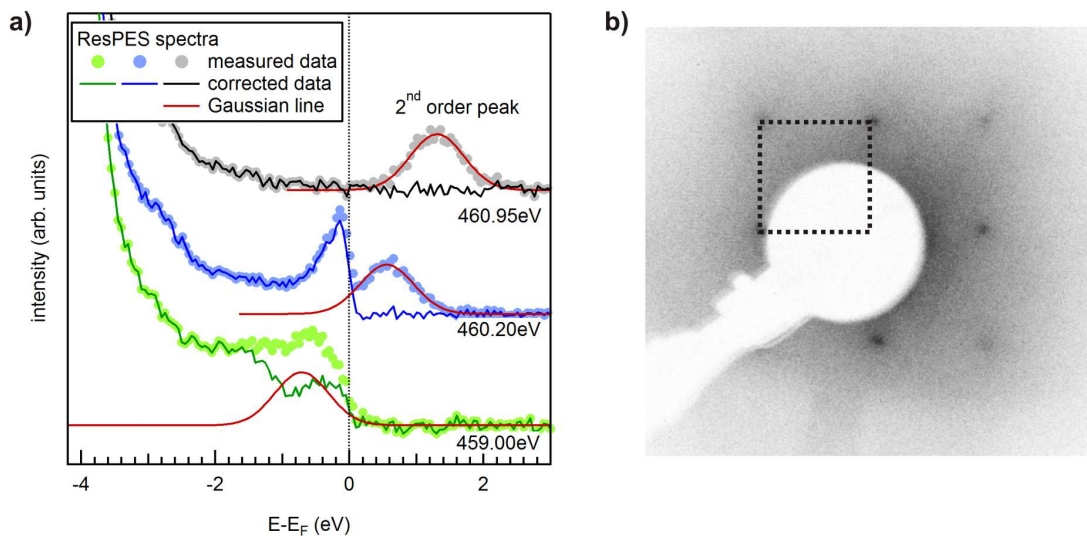


FIG. 6. (Color online) (a) Correction of the 2nd order light induced peak by subtraction of a Gaussian, exemplarily shown for spectra measured at 459.00 eV, 460.20 eV and 460.95 eV. (b) LEED pattern of a surface-cleaned LAO/STO sample at $E = 128.1$ eV showing a 1×1 surface structure. The lattice constant is 3.97 Å.